MOLECULAR AND CELLULAR BIOLOGY, Dec. 1996, p. 7072–7083 Vol. 16, No. 12
0270-7306/96/$04.00+0

Constitutive Activation of the *RON* Gene Promotes Invasive Growth but Not Transformation

MASSIMO M. SANTORO,[1,2] CHIARA COLLESI,[1] SILVIA GRISENDI,[1] GIOVANNI GAUDINO,[2] AND PAOLO M. COMOGLIO[1]*

Institute for Cancer Research, University of Turin Medical School, 10126 Turin,[1] and Department of Science and Advanced Technologies at Alessandria, 15100 Alessandria,[2] Italy

Received 18 June 1996/Returned for modification 25 July 1996/Accepted 20 September 1996

***MET*, *RON*, and *SEA* are members of a gene family encoding tyrosine kinase receptors with distinctive properties. Besides mediating growth, they control cell dissociation, motility ("scattering"), and formation of branching tubules. While there are transforming counterparts of *MET* and *SEA*, no oncogenic forms of *RON* have yet been identified. A chimeric Tpr-Ron, mimicking the oncogenic form of Met (Tpr-Met) was generated to investigate its transforming potential. For comparison, a chimeric Tpr-Sea was also constructed. Fusion with Tpr induced constitutive activation of the Ron and Sea kinases. While Tpr-Sea was more efficient than Tpr-Met in transformation, Tpr-Ron did not transform NIH 3T3 cells. The differences in the transforming abilities of Tpr-Met and Tpr-Ron were linked to the functional features of the respective tyrosine kinases using the approach of swapping subdomains. Kinetic analysis showed that the catalytic efficiency of Tpr-Ron is five times lower than that of Tpr-Met. Moreover, constitutive activation of Ron resulted in activation of the MAP kinase signaling cascade approximately three times lower than that attained by Tpr-Met. However, constitutive activation of Ron did induce a mitogenic-invasive response, causing cell dissociation, motility, and invasion of extracellular matrices. Tpr-Ron also induced formation of long, unbranched tubules in tridimensional collagen gels. These data show that *RON* has the potential to elicit a motile-invasive rather than a transformed phenotype.**

In human malignancies a number of tyrosine kinase receptors are constitutively activated by gene rearrangements that fuse their kinase domains with N-terminal unrelated sequences (for a review, see reference 46). The hepatocyte growth factor (HGF) receptor is converted into an oncogene by rearrangement of the *MET* proto-oncogene with a gene designated *TPR* (6). Similar rearrangements involving *TPR* have also been reported for *RAF* and *TRK* (19, 26). In Tpr-Met the extracellular, transmembrane, and part of the juxtamembrane domains of the HGF receptor are replaced by the N-terminal sequence of Tpr (36). The kinase activity of the resulting hybrid protein is deregulated, since two leucine-zipper motifs present in the Tpr moiety promote its constitutive dimerization (17, 41). This conformation mimics receptor activation following ligand binding.

A distinctive property of the HGF receptor (Met) is the ability to evoke a complex response including cell growth, "scattering," and tubulogenesis (for a review, see reference 5). Scattering involves cytoskeletal reorganization and loss of intercellular junctions, followed by active cell migration (14, 16, 55, 61). Epithelial tubulogenesis results from polarized cell growth and invasion of collagen matrices (33). These pleiotropic effects are elicited by the activation of several signalling pathways. Met-mediated signal transduction depends on ligand-induced phosphorylation of two critical carboxy-terminal tyrosine residues, which act as docking sites for multiple SH2-containing cytoplasmic effectors (37).

MET is the prototype of a gene family encoding structurally related receptors, including human *RON* (42) and avian *SEA* (25). The product of *RON* has been identified as the receptor for MSP (macrophage-stimulating protein; 13, 60). MSP was initially characterized as a macrophage chemotactic factor (49), but it actually exerts a wider spectrum of biological activities, mainly on epithelial and neuroendocrine cells (12). The human homolog of avian *SEA* and its specific ligand have not been identified. It has been demonstrated that Ron and Sea induce the same array of biological functions as Met: growth, scattering, and tubulogenesis. The multifunctional docking site responsible for Met signalling is conserved in the evolutionary related receptors, suggesting that this motif mediates the distinctive biological effects of the members of the family (32).

The oncogenic form of *SEA* (sarcoma, erythroblastosis, and anemia) has been identified as the transforming component of the avian erythroblastosis S13 retrovirus. The viral transforming gene encodes a 155-kDa transmembrane glycoprotein containing the extracellular and the transmembrane regions of the viral envelope protein fused with the *SEA* tyrosine kinase (22, 50).

Constitutively activated forms of *RON* have not been described. To ascertain its oncogenic potential, we generated a chimeric *TPR-RON* and transfected it in rodent fibroblasts. In spite of expressing a constitutive active form of the Ron tyrosine kinase, these cells were not transformed. However, Ron activation induced scatter and invasion of basement membranes in vitro. These data indicate that *RON* does not behave as a conventional proto-oncogene and suggest that its activation may be involved in progression toward the invasive phenotype.

MATERIALS AND METHODS

Molecular constructs. Cloning of *TPR-MET* cDNA has been reported previously (62). In this chimeric kinase, the first amino acid residue downstream from the recombination site is an aspartic acid (D-1010) conserved in *RON* (D-1027) and *SEA* (D-1031) sequences. *TPR-RON* and *TPR-SEA* constructs were obtained

* Corresponding author. Mailing address: Institute for Cancer Research, University of Turin Medical School, s.p. 142 Km 3.95, 10060 Candiolo (Turin), Italy. Phone: 39-11-993.3601. Fax: 39-11-993.3225.

by ligation of PCR-amplified fragments at the same junction site, in contiguity with the conserved D residue. For *TPR-RON* the forward primer was 5′-CCGC TTCTACCTCGAGGGCCGCTGCCAC-3′ designed on 5′ untranslated *TPR* sequence and the reverse primer was 5′-AGGAAAGATATCTGTTAAGTATT CAAGTTC-3, containing an *Eco*RV restriction site. The initial codon of the engineered *RON* intracellular segment corresponded to the conserved D-1027 residue. This was attained by amplification of the entire *RON* cDNA template (13), using the forward 5′-CATTCCCGGGCTGGATTCCACCA-3′ primer, containing a *Sma*I restriction site, and the reverse 5′-TCTGTGGAGTGAGGT ACCTAATG-3′ primer. For *TPR-SEA* the forward primer also matched the untranslated 5′ region of *TPR* (5′-AGCTCGAGAATTCGACATGGCGGCGG TGTTG-3′) and the reverse primer was 5′-AGGTCGACTGTTAAGTATTCA AGTTC-3′, containing a *Sal*I restriction site. A modified intracellular region of *SEA*, starting with the D-1031 residue, was generated by amplification of a partial chicken *SEA* cDNA (kindly provided by T. Parsons, Charlottesville, Va.), using the forward primer 5′-TGCTGCCTGTTGTCGACAGCCCTG-3′, containing a *Sal*I restriction site, and the reverse 5′-GGAATTCTCAGCGCACAGCCGCG TC-3′ primer. Tpr-Met/Tpr-Ron swapped constructs were prepared by using the chimeric cDNAs described above as templates. The recombination sites of the constructs bearing the swapped juxtamembrane subdomains were generated by the site-directed mutagenesis system (Promega, Madison, Wis.), inserting the *Tth*111I restriction site in position 644 of *TPR-MET*, with the oligonucleotide 5′-CTTCCTATGACTCGGTCATTGAAATGC-3′ and by exploiting the native *Tth*111I site at position 606 of *TPR-RON*. The following digestion and ligation resulted in the replacement of the tyrosine kinase and the C-terminal domains of Tpr-Met by the counterpart regions of Ron (Tpr-Ron.J_M). In parallel, the tyrosine kinase and C-terminal domains of Tpr-Ron were exchanged with the same regions of Tpr-Met (Tpr-Met.J_R). The constructs bearing the swapped C-terminal tails were obtained as follows. A *Sna*BI restriction site was inserted downstream from the kinase domain of *TPR-MET* (position 1446) and of *TPR-RON* (position 1533) by PCR amplification. The primer pairs were the forward 5′-G GGGAGCACTACGTACATGTGAAC-3′ and the reverse 5′-GTTCACATGT ACGTAGTGCTCCCC-3′ in the case of *TPR-MET*. The forward 5′-GGGGAC CATTACGTACAGCTGCCA-3′ and the reverse 5′-TGGCAGCTGTACGTA ATGGTCCCC-3′ primers were used in the case of *TPR-RON*. By recombination of the *Sna*BI restriction fragments, the swapping of the C-terminal tails of Tpr-Met and Tpr-Ron was obtained (Tpr-Ron.C_M and Tpr-Met.C_R). Finally, the tyrosine kinase domains were exchanged between Tpr-Met and Tpr-Ron, using the *Tth*111I restriction site of Tpr-Ron.C_M and Tpr-Ron.J_M to obtain the chimera Tpr-Ron.K_M and the *Eco*RV restriction site of Tpr-Met.C_R and Tpr-Met.J_R to obtain the chimera Tpr-Met.K_R. The fidelity of DNA amplification was verified by double-stranded DNA sequencing with T7 polymerase (Pharmacia, Uppsala, Sweden) according to the dideoxynucleotide methods (45). All constructs were inserted into the pMT2 eukaryotic expression vector, under control of the major late adenovirus promoter, and transiently expressed in COS-1 cells as well as in G418-selected NIH 3T3 mouse embryo fibroblasts.

Cell lines. NIH 3T3 mouse fibroblasts, MDCK cells, and COS-1 cells were purchased from the American Type Culture Collection. Cells were cultured in Dulbecco's modified Eagle's medium (DMEM) supplemented with 10% fetal calf serum (FCS) (Sigma Chemical Co., St. Louis, Mo.) and maintained at 37°C in a 5% CO_2-humidified atmosphere. NIH 3T3 fibroblasts and MDCK epithelial stable cell lines expressing the recombinant proteins were obtained by cotransfection of each recombinant plasmid cDNA with pSV2-neo plasmid (ratio of 15:1), using the calcium phosphate precipitation technique (CellPhect, Pharmacia, Uppsala, Sweden). The following selection was performed in growth medium supplemented with 0.8 mg of G418 sulfate (Geneticin; GIBCO BRL Life Technologies, Inc., Gaithersburg, Md.) per ml. After 2 weeks, the neomycin-resistant colonies were picked up and expanded into cell lines. Stable cell cultures expressing the respective recombinant proteins were selected by Western immunoblot and in vitro kinase assays, using specific C-terminal antisera. Met, Ron, and Sea antibodies were raised as described elsewhere (13, 32, 39).

Biochemical assays. Cells (3.5×10^6) were washed twice with cold phosphate-buffered saline (PBS) and lysed in an ice-cold buffer containing 10 mM PIPES [piperazine-*N*,*N*′-bis(2-ethanesulfonic acid)] (pH 6.8), 100 mM NaCl, 5 mM $MgCl_2$, 300 mM sucrose, 5 mM EGTA [ethylene glycol-bis(β-aminoethyl ether)-*N*,*N*,*N*′,*N*′-tetraacetic acid] (DIM buffer), 1% Triton X-100, 100 μM sodium orthovanadate, and inhibitors of proteases (aprotinin, 10 μg/ml; pepstatin, 10 μg/ml; leupeptin, 50 μg/ml; soybean trypsin inhibitor, 100 μg/ml; phenylmethylsulfonyl fluoride, 1 mM). The cell lysates were cleared by centrifugation at 15,000 × *g* for 15 min at 4°C. Equal amounts (800 μg) of total proteins from each cell lines, determined by using the BCA protein assay reagent kit (Pierce, Rockford, Ill.), were immunoprecipitated with stirring for 2 h at 4°C with the specific antisera (anti-Met, anti-Ron, anti-Sea, see above) adsorbed to 30 μl of protein A-Sepharose 4B packed beads (Pharmacia). The immunocomplexes were washed twice with lysis buffer, and proteins from immunoprecipitates were solubilized in boiling Laemmli buffer in reducing conditions. The proteins were separated on sodium dodecyl sulfate (SDS)–8% polyacrylamide gels and transferred to nitrocellulose filters (Hybond; Amersham). Filters were probed with the appropriate antibodies, and specific binding was detected by the enhanced chemiluminescence system (ECL; Amersham). The in vitro kinase assays were performed on immunocomplexes (as described above) by incubation in 50 μl of 25 mM HEPES (*N*-2-hydroxyethylpiperazine-*N*′-2-ethanesulfonic acid) (pH 7.4), 5 mM $MnCl_2$, 100 μM dithiothreitol (DTT), in the presence of 40 μM ATP and 10 μCi of [γ-^{32}P]ATP (specific activity, >5,000 Ci/mmol; Amersham) for 10 min at room temperature. The reaction was stopped by adding 1 ml of ice-cold lysis buffer containing 15 mM EDTA, and the labeled immunocomplexes were eluted in boiling Laemmli buffer. Labeled phosphoproteins were separated on SDS–8% polyacrylamide gels and analyzed by autoradiography. In vivo tyrosine autophosphorylation was evaluated by Western blotting using phosphotyrosine monoclonal antibodies from Upstate Biotechnology, Inc. (Lake Placid, N.Y.).

Transformation assays. The focus-forming assays were performed on NIH 3T3 fibroblasts (5×10^5 cells) that were cotransfected with 10 μg of each recombinant plasmid and 0.8 μg of pSV2-neo using the calcium phosphate precipitation technique (CellPhect; Pharmacia). Twenty-four hours after DNA transfection the cultures were split at low cell density into 100-mm-diameter dishes and incubated in DMEM supplemented with 5% FCS. The cell cultures were maintained at confluence and screened for focus formation 15 to 21 days later. Spontaneous formation of foci was negligible. To verify the efficiency of transfection, a fraction of cells were selected in G418-containing medium. Focus-derived cells and G418-resistant clones were established as stable lines, to verify chimeric protein expression. The in vitro transforming ability of all constructs was also assessed by a soft-agar assay using the NIH 3T3 pooled stable cell lines. Cells (3.0×10^3) were suspended in 1 ml of DMEM containing 10% FCS and 0.35% low gelling temperature agarose type VII (Sigma Cell Culture Reagents, St. Louis, Mo.) and quickly plated in six-well dishes onto a hardened base layer containing DMEM with 0.7% of agarose. Plates were fed with 1 ml of DMEM–10% FCS–0.35% agar at weekly intervals. The number of colonies with more than 30 cells was counted at 21 days. All the anchorage-independent growth experiments were performed in triplicate.

MAP kinase activity. NIH 3T3 pooled stable cells were serum deprived for 16 h, washed twice with cold PBS, and then lysed in 1 ml of an ice-cold buffer containing 50 mM HEPES (pH 7.5), 150 mM NaCl, 10% glycerol, 1% Triton X-100, 1.5 mM $MgCl_2$, 1 mM EDTA, 1 mM EGTA, 100 mM NaF, 100 μM sodium orthovanadate, 10 μg (each) of aprotinin and leupeptin per ml, and 1 mM phenylmethylsulfonyl fluoride. Lysates were cleared by centrifugation at 13,000 × *g* for 15 min at 4°C, and the protein concentration in the supernatant was determined using the micro-BCA protein assay reagent kit (Pierce). Aliquots (100 μg) of cell protein were immunoprecipitated with an anti-p42^{ERK2} polyclonal antiserum (TR2; kindly provided by M. J. Weber, Charlottesville, Va.) for 2 h at 4°C with stirring. The immunocomplexes were immobilized on protein A-Sepharose beads (40 μl of packed beads per 1 ml of lysate; Pharmacia) and washed extensively with lysis buffer followed by two washes with the kinase reaction buffer (25 mM Tris-HCl [pH 7.4], 40 mM $MgCl_2$, 1 mM DTT, 0.5 mM EGTA). The kinase assay was carried out in 50 μl of kinase reaction buffer containing 0.5 mg/ml of myelin basic protein (MBP) per ml, 200 μM ATP, and 3 μCi of [γ-^{32}P]ATP for 30 min at 30°C. The reaction was stopped by adding 50 μl of Laemmli sample buffer, and proteins were electrophoresed on SDS–15% polyacrylamide gels. Phosphorylated MBP was detected by autoradiography and by counting Cerenkov emissions of the excised bands.

Analysis of kinetic parameters. Equal amounts (10 μg) of Tpr-Met, Tpr-Ron, Tpr-Met.C_R, and Tpr-Ron.C_M cDNAs were transfected in COS-1 cells by the DNA-calcium phosphate coprecipitation procedure. After 60 h of transient transfection, the confluent cell cultures were placed on ice, washed twice with cold PBS, and solubilized in 1 ml of ice-cold DIM buffer containing 1% Triton X-100, 100 μM sodium orthovanadate, and inhibitors of proteases (aprotinin, 1 μg/ml; pepstatin, 50 μg/ml; leupeptin, 500 μg/ml; soybean trypsin inhibitor, 500 μg/ml; phenylmethylsulfonyl fluoride, 1 mM). Cell lysates were cleared by centrifugation at 4°C for 15 min at 13,000 × *g*. The supernatants were immunoprecipitated with Sepharose-protein A (70 μl of packed beads per ml of lysate) and with the relative antibodies (Ron antiserum was used at a concentration of 4 μl of cell lysate per ml, while Met antiserum was used at 10 μl/ml) for 3 h at 4°C with stirring. To quantify the relative amounts of protein immunoprecipitated by the same antibody from different samples, aliquots of immunocomplexes were saved and analyzed by Western blotting. After immunoprecipitation, beads were washed two times with lysis buffer and two times with the kinase buffer (25 mM HEPES-NaOH [pH 7.4], 5 mM $MnCl_2$, 100 μM DTT). The washed immunocomplexes were divided into aliquots and used for the experiments. To evaluate [K_m (ATP)], the kinase reaction was performed in 30 μl of reaction buffer supplemented with increasing concentrations of ATP (5, 10, 20, 40, and 80 μM) in autophosphorylation experiments. A constant concentration of MBP exogenous substrate (50 μM) was also present in exogenous substrate phosphorylation experiments. To measure catalytic efficiency, the kinase reaction was performed in the presence of increasing concentrations of MBP exogenous substrate (1.25, 2.5, 5, 10, and 20 μM) and of a constant concentration of ATP (100 μM). ATP concentration was adjusted to a specific activity of 0.5 to 0.6 μCi/mmol with [γ-^{32}P]ATP (Amersham). The range of ATP concentrations was determined by serial dilutions, maintaining the specific activity unchanged. The standard reaction time was 3 min at 4°C, with continuous stirring both for autophosphorylation and for exogenous substrate phosphorylation, as determined by preliminary time-course experiments. The reactions were stopped by adding boiling Laemmli buffer, and the eluted proteins were separated on SDS–8% polyacrylamide gels (autophosphorylation) or on SDS–15% polyacrylamide gels (myelin basic protein phosphorylation), followed by autoradiography at −70°C with intensifying

screens. Phosphate incorporation was estimated by scintillation counting of the excised labeled bands in a Packard beta counter.

Biological assays. To avoid clonal variations, in our analyses we used pooled populations of G418-selected NIH 3T3 cells as described above, rather than isolated and specific clones for the different biological assays. Parallel cultures of the NIH 3T3 cells stably transfected with the empty pSV2-neo vector were also established as control cell lines. For growth rate experiments, pooled NIH 3T3 transfectants (3.0×10^3 cells per well) were plated at low serum concentration (2% FCS) in 24-well plates, changing the medium every 2 days. Cell number was estimated after staining with crystal violet by a colorimetric assay (28). For each cell line and time point the experiments were conducted in quadruplicate. The assays for motility and matrix invasion (1) were performed in blind-well Transwell chambers (Costar Corporation, Cambridge, Mass.). Briefly, 10^5 cells of each NIH 3T3 pooled cell line were seeded on the upper side of a porous polycarbonate membrane (8.0-μm-pore size) coated (invasion assays) or not coated (cell migration assays) with the artificial basement membrane Matrigel (12.5 μg per filter; Collaborative Biomedical Products; Becton Dickinson Labware, Waltham, Mass.). Only cells able to migrate or with an invasive phenotype are able to move through the membrane and grow on the lower side of the filter. After 12 h of incubation (for migration assays) or 36 h (for invasion assays), cells attached to the upper side of the filters were mechanically removed, whereas cells that migrated or invaded the Matrigel were fixed with glutaraldehyde and stained with crystal violet. The stained cells that passed through the membrane pores were solubilized in 10% acetic acid and absorbance at 595 nm was counted in a microplate reader (Perkin-Elmer). Absorbance was converted into cell number by reference to a stained cell concentration standard curve for each cell type. Both assays were performed in the presence of low serum concentration (2% FCS).

Tubulogenesis assay. Pooled G418-selected clones of MDCK cells expressing Tpr-Met, Tpr-Ron, Tpr-Sea, Tpr-Ron.C_M, and Tpr-Met.C_R proteins at comparable levels were used for the biological assay. For the cotransfection experiments, two independent G418-selected clones of MDCK coexpressing Tpr-Met and Tpr-Ron at comparable levels were used. Parallel MDCK cells stably transfected with the empty vector were also established and used as control cell lines (mock transfected). The morphogenetic activity of the MDCK cultures was analyzed as described previously (33). Briefly, the cells were harvested from cultures by using trypsin-EDTA and suspended at a concentration of 10^5 cells per ml in collagen solution containing type I collagen gel (3 mg/ml; Collaborative Biomedical Products; Becton Dickinson Labware), 10× DMEM (Gibco BRL), and 0.5 M HEPES (pH 7.4). Aliquots (100 μl) of the cell suspension were dispensed in microtiter 96-well plates and allowed to gel for about 15 min at 37°C before adding 200 μl of DMEM supplemented with 10% FCS. The medium was changed every 2 days. After 7 to 10 days the morphogenic responses were evaluated.

RESULTS

Tpr-Ron is a constitutively active tyrosine kinase. *TPR-MET* results from a rearrangement between the 5′ region of *TPR* and the 3′ region of *MET*. In Tpr-Met the Met sequence starts with an aspartic acid within the juxtamembrane domain. In the rearranged viral *ENV-SEA*, the Sea sequence begins with the same conserved aspartic acid residue. Thus, we generated recombinant Tpr-Ron and Tpr-Sea by using the same boundary (Fig. 1A). The cDNAs were stably expressed in NIH 3T3 fibroblasts. To avoid clonal variations, all experiments were performed on pooled G418-resistant colonies, rather than on isolated clones. The expression of recombinant chimeras was analyzed in stable transfectants by immunoprecipitation and Western blotting, using excess C-terminal antisera to circumvent differences in affinity. All chimeras were found to be expressed at comparable levels (Fig. 2A). The level of tyrosine phosphorylation of the Tpr chimeras in intact cells was assessed by immunoprecipitation followed by Western blotting with antiphosphotyrosine antibodies. Their in vitro enzymatic activities were examined by kinase assay. All chimeric proteins showed high levels of autophosphorylation on tyrosine and were capable of autokinase activity (Fig. 2A). The chimeric proteins migrated according to an apparent molecular mass of 65 kDa for Tpr-Met and of 60 kDa for Tpr-Ron and Tpr-Sea. These variations can be explained by differences in molecular mass and/or by the presence of 14 potential phosphorylation sites in Tpr-Met versus 12 in Tpr-Ron and Tpr-Sea. Phosphorylation is known to influence protein migration in SDS-polyacrylamide gels.

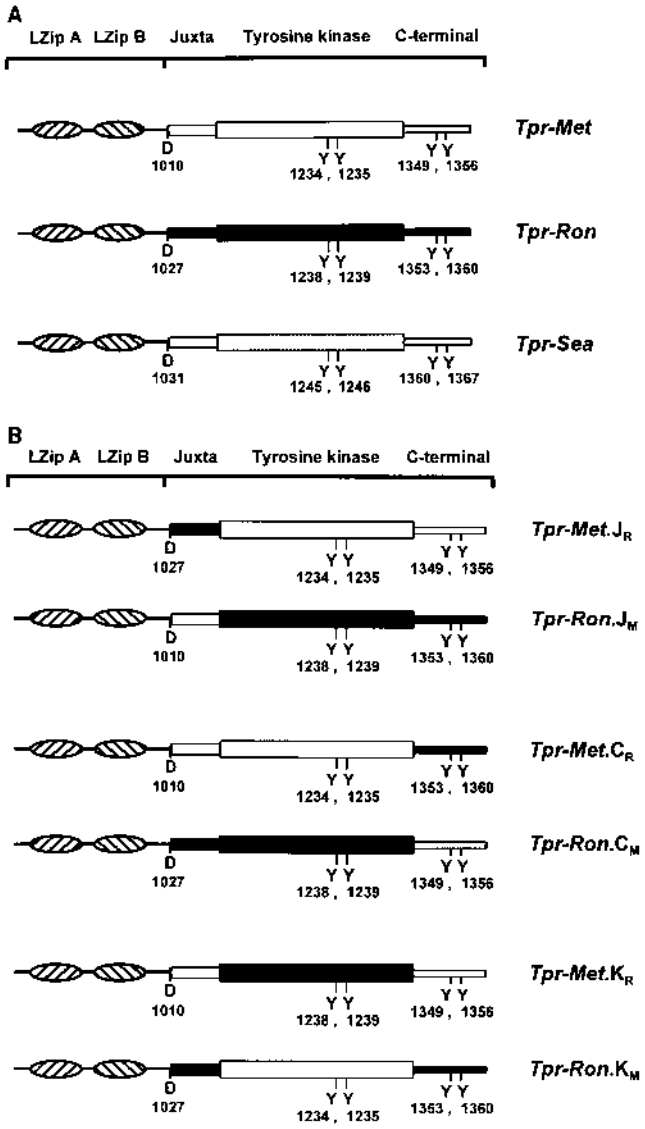

FIG. 1. (A) Schematic representation of the chimeric proteins containing Tpr and the intracellular domains of Met, Ron, and Sea. The leucine zipper motifs (LZipA and LZipB) and the receptor intracellular subdomains are indicated at the top. Fusion with Tpr occurs at an aspartic acid residue (D), conserved in Met, Ron, and Sea. The two neighboring tyrosine residues (Y) of the kinase domains, corresponding to the major autophosphorylation site and the tyrosine of the C-terminal tails in the conserved bidentate multifunctional docking site, are shown. (B) Schematic representations of Tpr-Met and Tpr-Ron swapped chimeras. Acronyms on the right identify the different constructs. In the upper two constructs, the juxtamembrane (J) subdomains are replaced. Tpr-Met.J_R contains the Ron juxtamembrane subdomain and Tpr-Ron.J_M contains that of Met. In the middle two constructs the carboxy-terminal (C) tails are exchanged. Tpr-Met.C_R contains the Ron tail and Tpr-Ron.C_M contains that of Met. In the lower two constructs the kinase (K) domains are exchanged. Tpr-Met.K_R contains the kinase domain of Ron and Tpr-Ron.K_M contains that of Met. The Tpr, Met, and Ron sequences are identified by hatched, white, and black areas, respectively.

Tpr-Ron does not transform rodent fibroblasts. Tpr-Met, Tpr-Ron, and Tpr-Sea were tested in a focus-forming assay by transfection in rodent fibroblasts. The efficiency of transfection was assessed by cotransfection with pSV2-neo. The number of G418-resistant colonies obtained was the same for the three Tpr chimeras. Cells transfected with Tpr-Sea yielded a twofold higher frequency of focus formation than those transfected

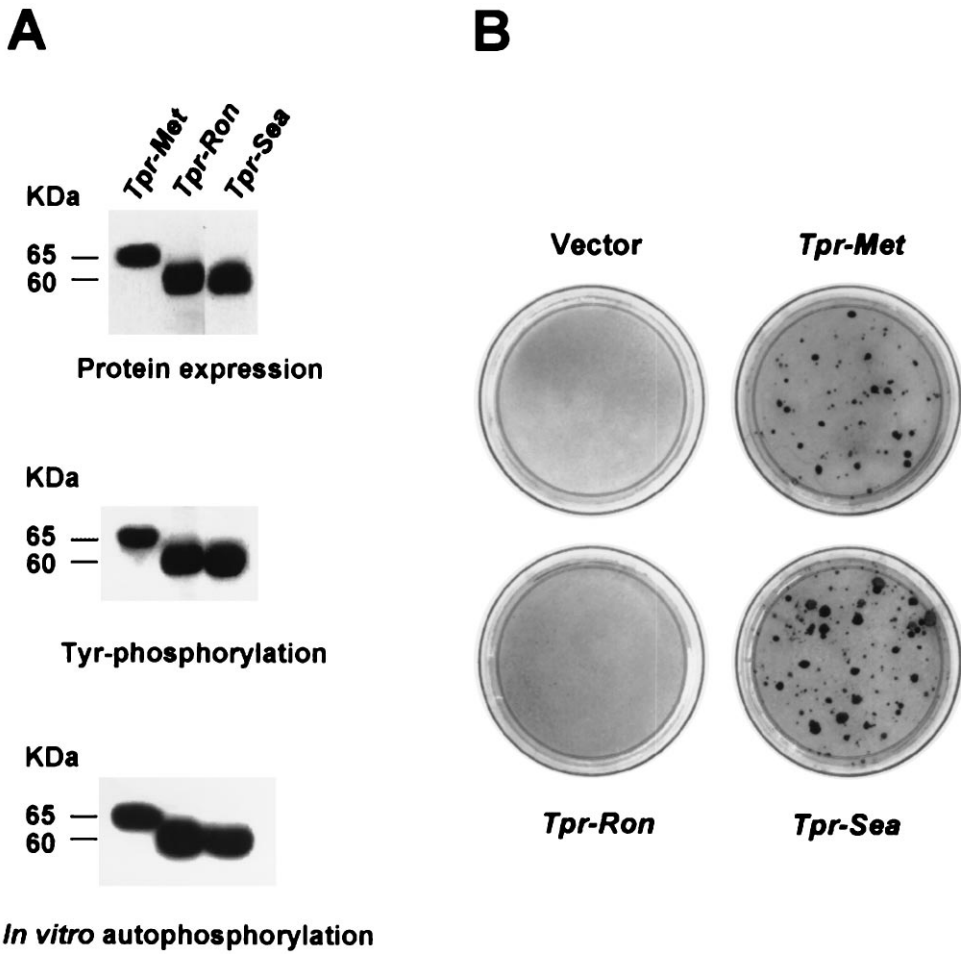

FIG. 2. Constitutive activation and transforming ability of the Tpr chimeras. (A) Protein expression, in vivo autophosphorylation, and in vitro tyrosine kinase activity of Tpr-Met, Tpr-Ron, and Tpr-Sea. The specific chimeras were analyzed by immunoprecipitation and Western blotting with antibodies against the C-terminal domains of Met, Ron, and Sea (Protein expression) and with anti-phosphotyrosine antibodies (Tyr-phosphorylation). The in vitro tyrosine kinase activity of the chimeras was tested by incubating specific immunoprecipitates with [γ-^{32}P]ATP (In vitro autophosphorylation). (B) Focus-forming assay of rodent fibroblasts transfected with the three Tpr chimeras. Tpr-Met showed a focus-forming activity of 290 ± 30 foci per 10 μg of cDNA transfected. Tpr-Sea induced twice as many foci as Tpr-Met. No foci were scored in Tpr-Ron or cells transfected with vector alone. Dishes were stained with crystal violet. The figure is representative of at least three independent transfections performed in triplicate.

with Tpr-Met. Unexpectedly, Tpr-Ron was completely unable to induce foci of transformation (Fig. 2B). Selected clones of transfected cells, expressing levels of Tpr-Ron at least threefold over the unselected population pool, did not form foci at confluence. This ruled out the possibility that lack of transformation was due to low expression of the chimeric protein.

As an alternative approach to investigate the transforming potential of the *MET* gene family, we performed anchorage-independent growth assays on fibroblasts expressing the three Tpr-chimeras. Tpr-Met stable transfectants grew in soft agar, yielding a significant number of colonies. Tpr-Sea transfectants yielded twice as many colonies. In contrast Tpr-Ron transfectants failed to develop anchorage-independent colonies (Table 1).

Tpr-Ron activates the mitogenic pathway. Cell transformation requires a strong mitogenic signal for which MAP kinase phosphorylation is a mandatory step (7). MAP kinase activation in pooled stable NIH 3T3 transfectants was analyzed by measuring phosphorylation of an exogenous substrate after immunoprecipitation with anti-MAP kinase antibodies (Fig. 3). In cells expressing Tpr-Sea and Tpr-Met, the MAP kinase was activated seven- and sixfold over the background, respec-

TABLE 1. The in vitro transforming ability of Tpr-Met, Tpr-Ron, and Tpr-Sea

Cell transfected with:	No. of colonies in soft agar[a]	Focus-forming activity[b]
Mock	<1	<0.01
Tpr-Met	12 ± 3	1.00
Tpr-Ron	<1	<0.01
Tpr-Sea	29 ± 3	1.92
Tpr-Met.C_R	28 ± 2	1.96
Tpr-Ron.C_M	<1	<0.01
Tpr-Met.J_R	11 ± 3	0.95
Tpr-Ron.J_M	<1	<0.01
Tpr-Met.K_R	<1	<0.01
Tpr-Ron.K_M	26 ± 1	1.90

[a] Cells were seeded at a density of 3.0×10^3 per well, and the number of colonies (>30 cells in size) was scored after 3 weeks. Numbers indicate the averages (± standard deviation) of three independent experiments performed in triplicate.

[b] Values were determined as ratios between the number of observed foci and the number of G418-resistant colonies. The values were normalized to the focus-forming activity of Tpr-Met, which was set at 1.00. Numbers were calculated from the results of at least three independent transfections of each construct.

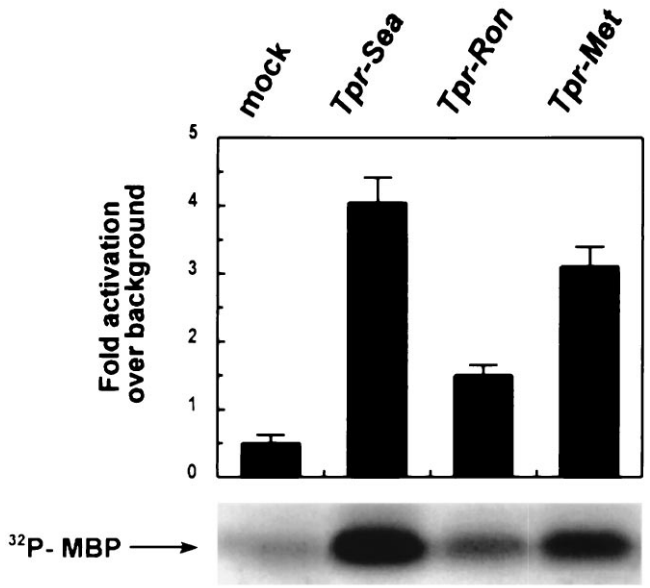

FIG. 3. MAP kinase activation by Tpr-Sea, Tpr-Ron, and Tpr-Met. The assay was performed by measuring the amount of ^{32}P transferred to myelin basic protein (MBP) by MAP kinase immunoprecipitated with anti-$p42^{ERK2}$ antibodies. MAP kinase activation is expressed as fold increase over the background in triplicate determinations (bars = standard deviations). Tpr-Sea and Tpr-Met showed more than a twofold increase over Tpr-Ron in MAP kinase activation.

tively, while expression of Tpr-Ron resulted in only a modest increase of MAP kinase activity. This MAP kinase stimulation, however, was significant and correlated with induction of cell proliferation (Fig. 4). Cells expressing Tpr-Met or Tpr-Sea acquired a transformed behavior characterized by unrestrained proliferation. Cells expressing Tpr-Ron were able to grow in low serum, but their growth was arrested when saturation density was reached (contact-arrested condition). Tpr-Met- and Tpr-Sea-transformed cells were spindle shaped, elongated, and highly refractile. Cells expressing Tpr-Ron were poorly refractile and highly adherent, typical of normal fibroblasts (unpublished data).

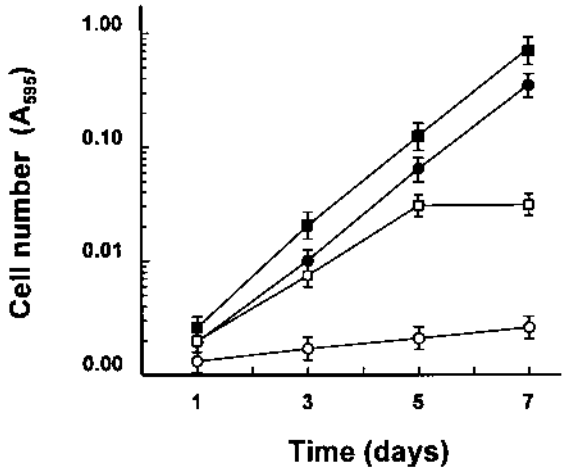

FIG. 4. Cell proliferation induced by Tpr-Met, Tpr-Ron, and Tpr-Sea. NIH 3T3 cells expressing the Tpr chimeras were grown in low serum concentration (2% FCS). The cell number was evaluated by absorbance (A_{595}) of monolayer stained with crystal violet and solubilized. The data shown are the averages (bars = standard deviations) of replicate wells ($n = 3$) from a typical experiment. Cells expressing transforming Tpr-Met (●) and Tpr-Sea (■) displayed a fast and unrestrained proliferation. Cells expressing Tpr-Ron (□) showed an increased growth rate over the vector-alone control cells (○) and reached a saturation density, corresponding to a contact-arrested condition. These data are representative of at least three independent experiments.

Transformation is linked to the functional features of kinase domains. To understand why constitutive activation of Ron does not result in cell transformation we swapped specific Ron subdomains with the corresponding Met regions. The Ron subdomains exchanged with Met were (i) the juxtamembrane domain (amino acids [aa] 1027 to 1085), which contains several serine residues, putative targets for negative regulation (11); (ii) the kinase domain (aa 1085 to 1352); and (iii) the carboxy-terminal tail (aa 1353 to 1400), which includes the multifunctional docking site essential for signal transduction (37). The structure of the swapped recombinant proteins and the acronyms used to identify them are illustrated in Fig. 1B. The recombinant proteins were all expressed with the same efficiency, were equally capable of autophosphorylation on tyrosine in vivo, and displayed comparable kinase activity in vitro (Fig. 5A).

The transforming potential of swapped Tpr chimeras was analyzed in focus-forming and soft agar growth assays. Substitution of the Ron juxtamembrane domain with that of Met (Tpr-Ron.J_M) did not confer transforming ability to Tpr-Ron. In the complementary experiments, the transforming ability of Tpr-Met was unchanged by the replacement of its juxtamembrane subdomain with that of Ron (Tpr-Met.J_R). Replacement of the Ron carboxy-terminal tail with that of Met (Tpr-Ron.C_M) did not confer transforming ability to Tpr-Ron. Unexpectedly, the mirror construct Tpr-Met, containing the carboxy-terminal tail of Ron (Tpr-Met.C_R), yielded a twofold higher number of foci. These results were confirmed by similar chimeras for which the tyrosine kinase was the domain being swapped. The Tpr-Met construct having its kinase domain replaced by that of Ron (Tpr-Met.K_R) did not induce foci of transformation. Conversely, Tpr-Ron under the control of the Met kinase was as active as Tpr-Met.C_R (Fig. 5B).

Similar results were obtained when the swapped chimeras were tested for anchorage-independent growth (Table 1). Altogether, these experiments show that the transforming ability of Tpr-Ron and Tpr-Met is linked to their kinase domains, whose intrinsic properties must be different.

Catalytic efficiency of the Ron kinase. To evaluate the catalytic efficiency of Tpr-Met and Tpr-Ron we determined the kinetic parameters for tyrosine autophosphorylation and for phosphorylation of the exogenous substrate MBP. The assays were performed in the presence of 5 mM Mn^{2+} (35) at time points and temperatures optimized for a linear response, as described in Materials and Methods.

The apparent Michaelis-Menten constants [K_m (app)] of Tpr-Met and Tpr-Ron for ATP were found similar both in autophosphorylation (2.36 ± 1.0 μM and 2.32 ± 0.5 μM, respectively) and in phosphorylation of the MBP exogenous substrate (10.0 ± 0.5 μM and 10.6 ± 0.6 μM, respectively). These values are in the same range as those previously published for the full-size Met receptor kinase (35) and for the full-size Ron receptor (unpublished data).

Similarly, the apparent Michaelis-Menten constant of Met and Ron kinases for MBP was in the same order of magnitude (Table 2).

However, when the V_{max} (maximum rate of metabolism) for MBP exogenous substrate phosphorylation was measured, a significant difference between the Met kinase and the Ron kinase was observed. The catalytic efficiency of the Ron kinase, calculated as V_{max}/K_m (24), was found to be five times lower than the efficiency of the Met kinase (Table 2). Tpr-Met was

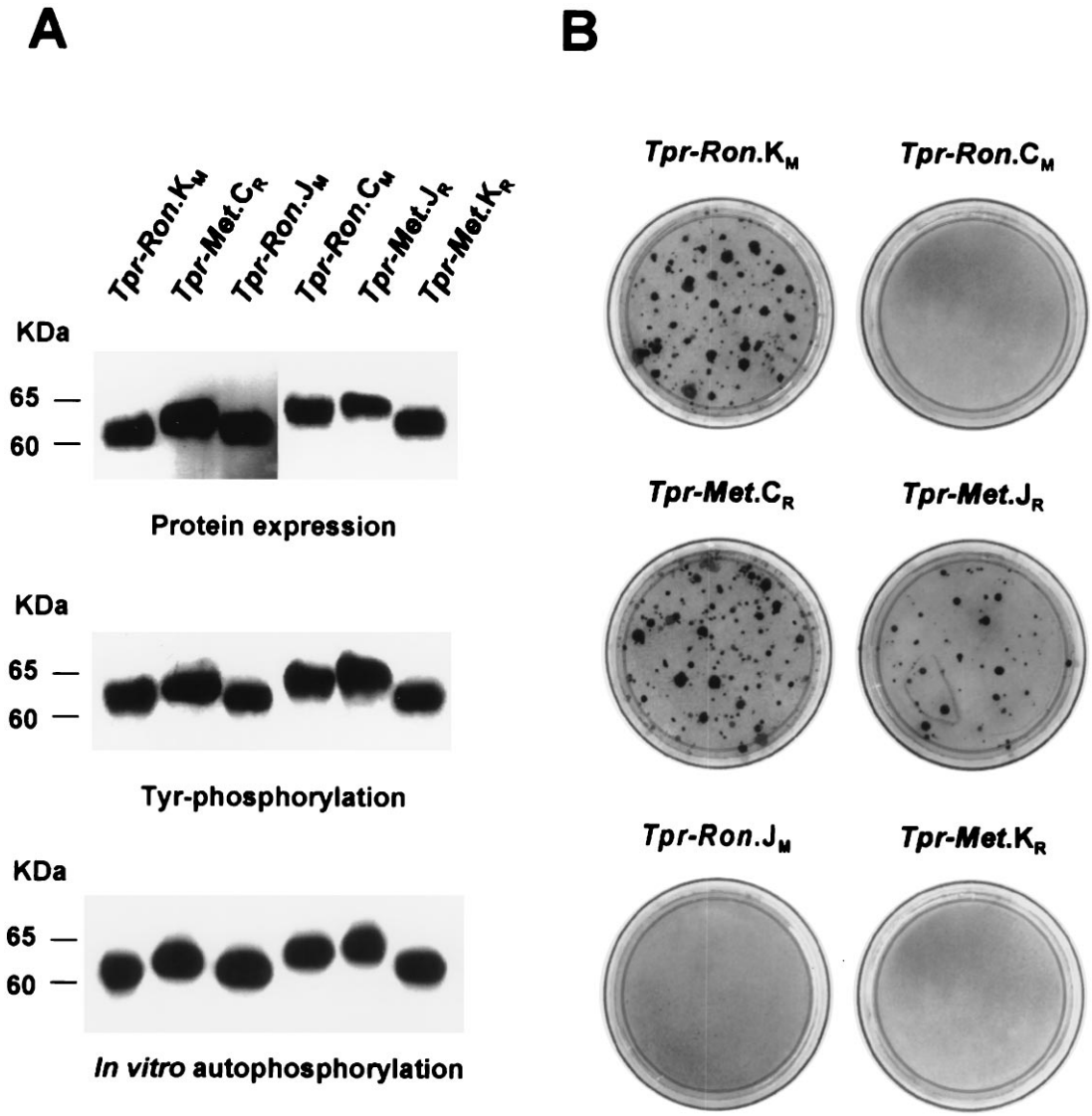

FIG. 5. Constitutive activation and transforming ability of the swapped chimeras between Tpr-Met and Tpr-Ron. (A) Protein expression, in vivo autophosphorylation, and in vitro tyrosine kinase activities of Tpr-Met and Tpr-Ron swapped chimeras. The specific chimeras were analyzed by immunoprecipitation and Western blotting with antibodies against the C-terminal domains of Ron (Tpr-Met.C_R, Tpr-Ron.J_M, and Tpr-Ron.K_M) and Met (Tpr-Ron.C_M, Tpr-Met.J_R, and Tpr-Met.K_R) (Protein expression) and with anti-phosphotyrosine antibodies (Tyr-phosphorylation). The in vitro tyrosine kinase activity of the chimeras was tested by incubating specific immunoprecipitates with [γ-^{32}P]ATP (In vitro autophosphorylation). (B) Focus-forming assay of rodent fibroblasts transfected with the swapped chimeras. Tpr-Met.C_R and Tpr-Ron.K_M induced twice as many foci as Tpr-Met.J_R. No foci were scored in Tpr-Ron.J_M, in Tpr-Ron.C_M, and in Tpr-Met.K_R transfected cells. Dishes were stained with crystal violet. The figure is representative of at least three independent transfections, performed in triplicate.

TABLE 2. Catalytic efficiency of Tpr-Met and Tpr-Ron[a]

Chimera	K_m (app) (μM)	V_{max} (app) (pmol/min)	V_{max} (app)/ K_m (app)
Tpr-Met	1.76 ± 0.5	1.15 ± 0.07	0.65
Tpr-Ron.C_M	1.79 ± 0.3	0.24 ± 0.01	0.13
Tpr-Ron	1.67 ± 0.5	0.44 ± 0.04	0.26
Tpr-Met.C_R	2.00 ± 0.2	2.46 ± 0.07	1.23

[a] Kinase assays were carried out on immunocomplexes, in the presence of increasing concentrations of MBP and of a constant concentration of ATP, as described in Materials and Methods. The kinase affinity for MBP [K_m (app)] and the phosphorylation maximal rate [V_{max} (app)] are indicated. The ratio V_{max} (app)/K_m (app) represents the catalytic efficiency of the enzyme.

compared with the swapped chimera bearing the Ron kinase domain fused with the tail of Met (Tpr-Ron.C_M) and Tpr-Ron was compared with that bearing the Met kinase fused with the tail of Ron (Tpr-Met.C_R). This rules out the possibility that the observed values reflected differences in affinities of the anti-Met and anti-Ron antisera used to immunoprecipitate the kinases, as in the case of the direct comparison between Tpr-Met and Tpr-Ron.

The kinetic curves showed that the reactions catalyzed by the two Tpr chimeras bearing the Ron kinase (Tpr-Ron and Tpr-Ron.C_M) attained saturation values consistently lower than those reached by the Met kinase (Fig. 6).

Activation of Ron induces an invasive phenotype. As shown above, constitutive activation of Ron triggers the MAP kinase pathway and cell proliferation but not transformation. We next

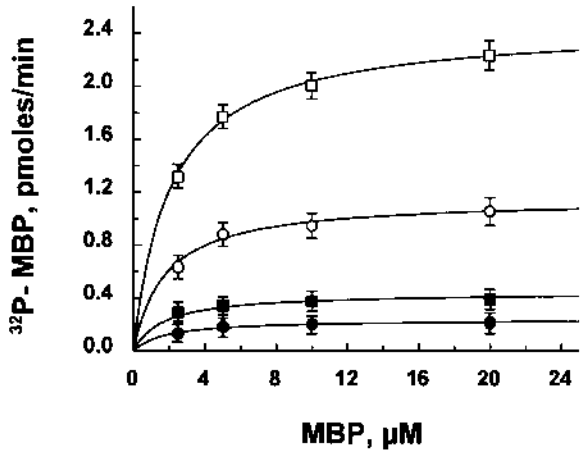

FIG. 6. Phosphorylation kinetics of the Ron (● and ■) and Met (○ and □) kinases in the presence of increasing concentrations of exogenous substrate (MBP). To immunoprecipitate identical amounts of active kinase, the swapped chimeras were used. Tpr-Ron (■) and Tpr-Met.C_R (□) were immunoprecipitated with anti-Ron antibodies; Tpr-Met (○) and Tpr-Ron.C_M (●) were immunoprecipitated with anti-Met antibodies. The V_{max} of the phosphorylation reaction by the Met kinase is fivefold higher than that of the Ron kinase. Plotted values are means of triplicate determinations (error bars). The kinetic curves were calculated by using a curve-fitting computer program for the Michaelis-Menten equation (GraFit; Microsoft).

investigated the other arm of the biological response: cell dissociation, motility, and invasiveness.

MDCK (Madin-Darby canine kidney) cells in cultures form tight epithelial monolayers with junctional complexes. HGF-induced activation of Met in these cell causes the breakdown of intercellular junctions and the transition to a fibroblastoid morphology, followed by cell motility (55). Expression of Tpr-Ron in MDCK cells resulted in a constitutive scattered phenotype (Fig. 7). The same phenotype was observed upon transfection of Tpr-Met and was indistinguishable from that occurring in MDCK cells bearing an HGF-dependent autocrine circuit (58). In contrast, Tpr-Sea did not induce any constitutive cell scattering (unpublished data).

NIH 3T3 fibroblasts expressing Tpr-Ron showed enhanced migration through 8.0-μm-pore-size polycarbonate filters. These cells were also capable of invasive migration through an artificial basement membrane made mainly of laminin, collagen IV, and heparan sulfate (Matrigel) (1). The cell migration and matrix invasion rates were comparable to those induced by transfection of Tpr-Met. Interestingly, cells expressing Tpr-Sea displayed only a modest increase in cell motility as well as in matrix invasion with respect to controls (Fig. 8).

These data demonstrate that constitutive activation of Ron, despite the low efficiency of its kinase, steers cells toward unrestricted cell dissociation, migration, and invasion.

Tpr-Ron induces unbranched tubulogenesis. MDCK cells are a sensitive target for signals controlling polarized growth. When stimulated in vitro by HGF or MSP, they migrate in tridimensional collagen gels and form long and branched tubules (32, 33).

MDCK cells expressing Tpr-Ron, seeded in tridimensional collagen gels, formed round cystic colonies within 3 to 5 days. Thereafter, the cysts developed a few spikes which, in a week, evolved into long tubular structures. Interestingly, these tubules never branched, unlike those observed in mock-trans-

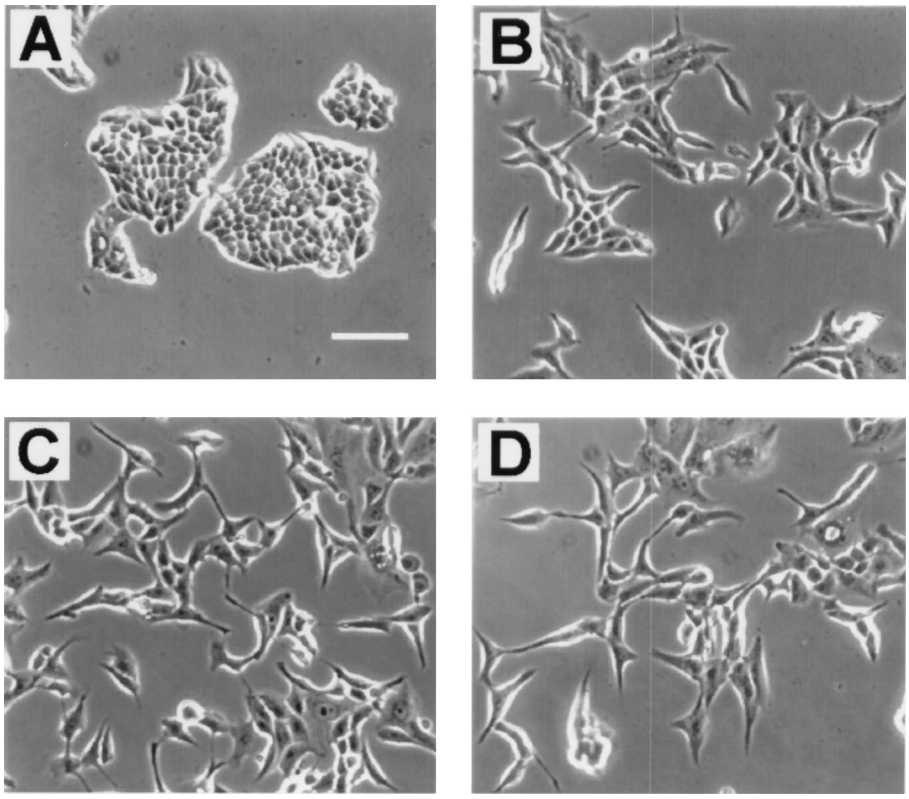

FIG. 7. Expression of Tpr-Met and Tpr-Ron in MDCK cells induces constitutive scattering. (A) Mock-transfected MDCK cells form tightly packed islands. (B) The islands dissociate and scatter in the presence of HGF (50 ng/ml). (C) MDCK cells express constitutively activated Tpr-Ron. (D) MDCK cells express constitutively activated Tpr-Met. Pictures were taken at the same magnification. Scale bar, 100 μm.

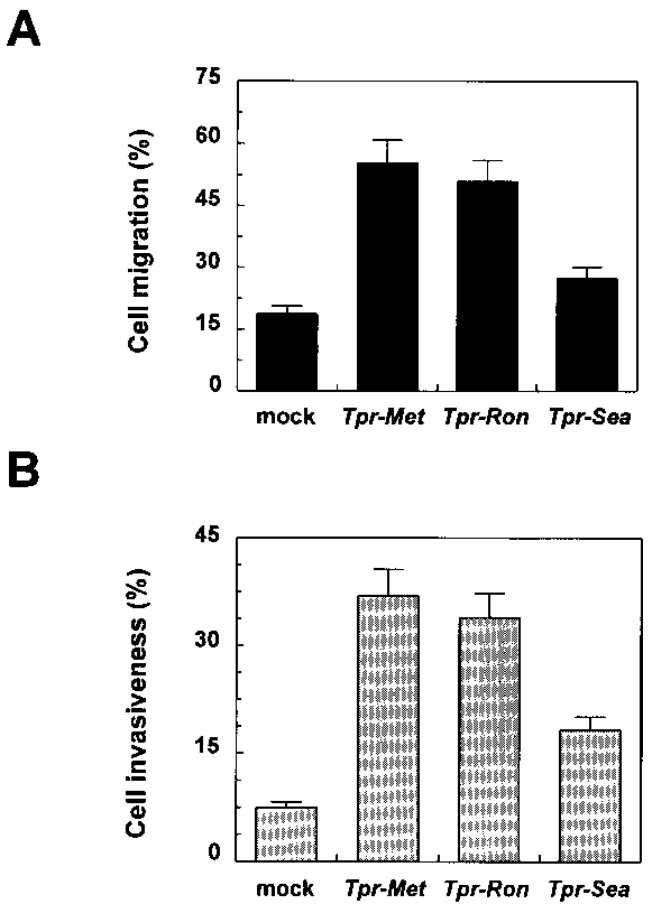

FIG. 8. Motility and matrix invasion of NIH 3T3 cells expressing Tpr chimeras. (A) Cell migration through 8.0-μm-pore-size filters of the Transwell chamber. (B) Cell invasiveness measured as migration through the filters coated with a reconstituted basement membrane made of laminin, collagen IV, and heparan sulfate. Controls were cells transfected with an empty vector (mock). Cell migration and invasiveness were expressed as the percentages of input cells that have migrated or have invaded the artificial basement membrane. Bars indicate the standard deviations of three independent experiments.

fected cells stimulated with HGF. On the other hand, MDCK cells expressing Tpr-Met and Tpr-Sea grew as larger spherical cysts, which never evolved into tubular structures. Also, the Tpr-Met.C_R chimera did not induce tubules in MDCK cells, but formed large cysts as well, whereas the counterpart construct, Tpr-Ron.C_M, led to unbranching morphogenesis, as did Tpr-Ron.

Moreover, MDCK cells cotransfected with Tpr-Met and Tpr-Ron constructs developed typical cystic structures with outward-projecting spikes. These spikes never developed a tubule formation (Fig. 9).

These data demonstrate that constitutive activation of Ron and Met kinases differentially induces the morphogenic program, independently from the nature of the transducing multifunctional docking sites.

DISCUSSION

Ligand-dependent activation of the Ron receptor induces cell proliferation under physiological conditions (13, 32, 59). However, naturally occurring oncogenic counterparts of *RON* have not been identified so far, nor is it known if *RON* has transforming potential in experimental conditions. Here we show that constitutive activation of the Ron tyrosine kinase, obtained by fusion with Tpr, stimulates MAP kinase and cell growth but does not transform NIH 3T3 fibroblasts. Since Tpr-Met is instead a powerful oncogene, we used chimeras obtained by swapping subdomains to identify the structural features responsible for this difference in transforming ability. Transforming assays performed on Tpr-Met and Tpr-Ron kinase-swapped chimeras indicate that the lack of Ron oncogenic potential is intrinsic to its tyrosine kinase domain. The integrity of the glycine loop motif involved in ATP binding is known to be critical for transformation mediated by $p60^{c\text{-}src}$ and *ErbB* (27, 47). For this reason, we tested the affinity of Tpr-Ron and Tpr-Met for ATP binding. Their K_m (ATP) values were found to be comparable.

There are several reports showing that the oncogenic potential of a tyrosine kinase is dramatically influenced by differences in the catalytic efficiency. In the case of the EGF receptor the transforming potential is unleashed by a single point mutation in the kinase domain, responsible for increased catalytic activity (48). The transforming properties of a number of $pp60^{c\text{-}src}$ mutants directly correlate with the degree of elevation of their catalytic activities (26). Moreover, the proto-oncogene *Neu* shows a lower V_{max} with respect to its oncogenic counterpart (29). Finally, the EGF receptor kinase has a V_{max} that is only threefold lower than the V_{max} of the oncogenic v-*erbB* (34). The reported data show that the catalytic efficiency of Tpr-Ron, expressed as a ratio between the V_{max} and the K_m (MBP), is five times lower than the V_{max} of Tpr-Met. This suggests that catalytic efficiency may be the parameter that discriminates between the oncogenic potentials of the two kinases.

As an estimate of the overall signalling ability of Tpr-Ron in vivo, we determined the level of activation of the MAP kinase cascade in NIH 3T3 cells stably expressing the three constructs. The total MAP kinase activity in cells expressing Tpr-Ron was significantly lower than that measured in cells expressing Tpr-Met and Tpr-Sea. This indicates that, in spite of the presence of an optimal multifunctional docking site, the relatively low catalytic efficiency of Tpr-Ron results in less effective signalling. We conclude that the downstream signalling cascade initiated by the permanently activated Ron, unlike that triggered by activation of Met and Sea, cannot overcome the negative mechanisms regulating growth at confluence and cannot sustain the critical threshold necessary for a fully transformed phenotype, at least in the system studied here. However, we cannot exclude the possibility that the *RON* gene displays transforming potential in other cell types, such as hemopoietic or neuroendocrine lineages that are known to express the Ron protein and that might respond to a lower threshold of MAP kinase signaling.

It has been demonstrated that quantitative differences in MAP kinase activation result in qualitative differences in gene expression and, consequently, in distinct biological responses (proliferation versus differentiation; 31). The intensity and duration of MAP kinase activation determine the different levels of phosphorylation and activation of transcription factors (9, 56, 57). An example of how the intensity of intracellular signals can produce large differences in transcriptional responses is given by the tyrosine kinase receptor Toll (44). Its differential activation leads to the generation of dorsoventral polarity in *Drosophila* embryos by controlling phosphorylation of the transcriptional factor dorsal at different levels (23, 54).

We ruled out the possibility that Tpr-Ron signaling involves specific effectors different from those recruited by Tpr-Met on the basis of the experiments performed with the C-terminal swapped chimeras. Surprisingly, the Ron C-terminal tail was

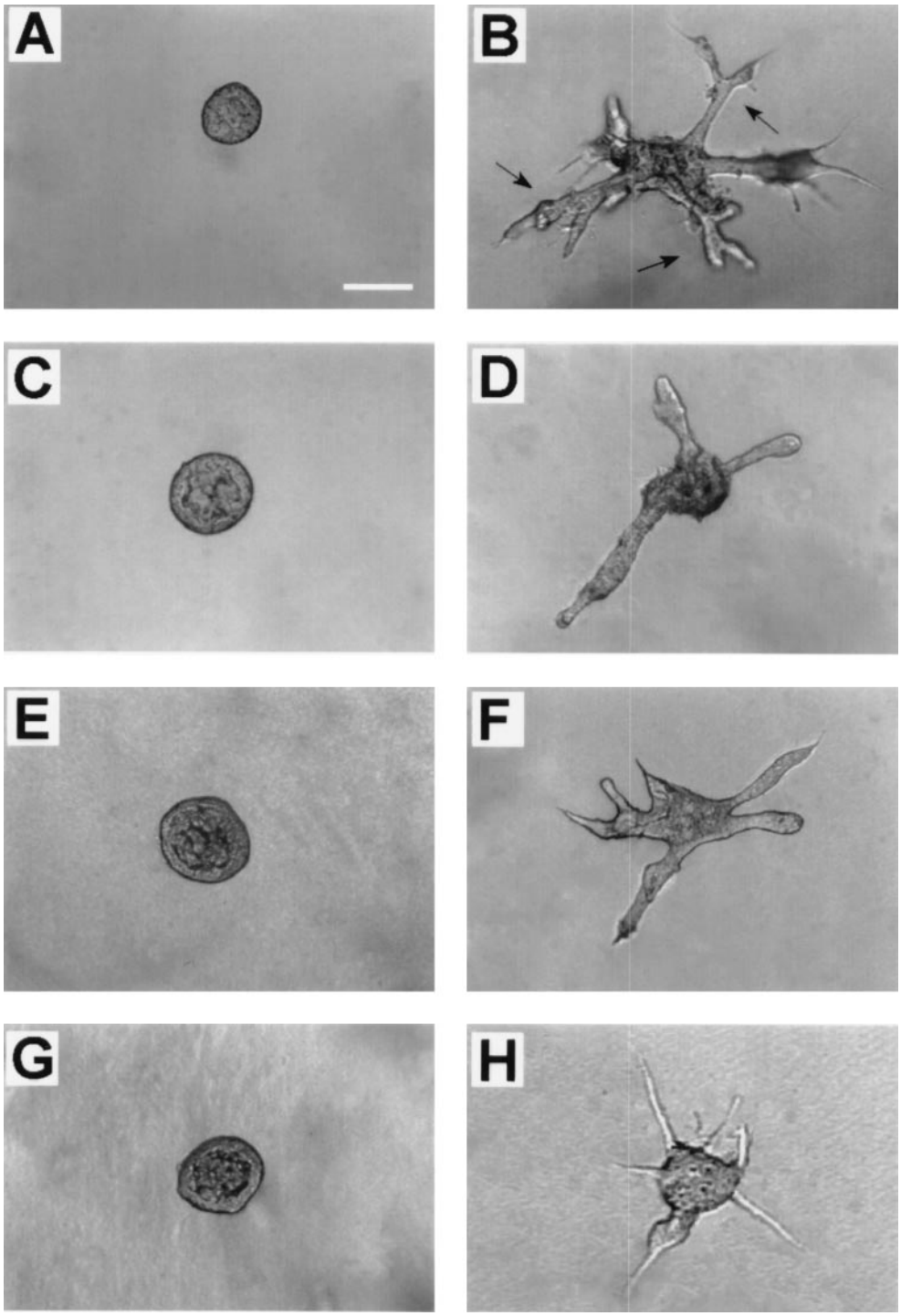

FIG. 9. Growth in tridimensional collagen matrix of MDCK cells expressing Tpr-Ron and Tpr-Met. (A) Mock-transfected cells growing as spherical cysts. (B) Mock-transfected cells in the presence of 100 ng of HGF per ml. Branching tubular structures are observed (arrows). (C, E, and G) Cells expressing Tpr-Met, Tpr-Sea, and Tpr-Met.C_R, respectively. Formation of tubules is completely inhibited. (D and F) Cells expressing Tpr-Ron and Tpr-Ron.C_M, respectively, forming long and unbranched tubules. (H) Cells coexpressing Tpr-Met and Tpr-Ron. Few spikes projecting outward never developed tubular structures. Micrographs of representative fields were taken 1 week after seeding single-cell suspensions. Scale bar, 100 μm.

found to be even better than the Met tail in inducing cell transformation. The Ron tail includes the conserved multifunctional docking site (Y-1353 VQL-X_3-Y-1360 MNL) that binds in vitro the same set of SH2-containing signal transducers bound by Met (Y-1349 VHV-X_3-Y-1356 VNV) (37). It has been shown that the transforming potential of Tpr-Met correlates with the level of Met-mediated Ras activation, which in turn depends on the ability to bind Grb-2 (10, 38). The Met receptor binds Grb-2 and activates the Ras guanyl-nucleotide exchanger Sos (18) through the Y-1356 V<u>N</u>V sequence (i.e.,

the phosphotyrosine followed by an asparagine residue in the +2 position) (37). Similarly, the Ron tail can recruit the Grb-2-Sos complex (30) through Y-1360 MNL (53). The reason for the enhanced efficiency of transformation displayed by the Ron tail (once fused to Tpr-Met) is thus not easily explained. The tyrosine of the Ron Grb-2 binding site may be a better substrate for phosphorylation than the corresponding tyrosine of Met, as it is followed by a residue with a larger hydrophobic side chain at the +1 position (Y-1360 MNL; 51). On the other hand, Tpr-Sea had a transforming ability better than Tpr-Met. In this case the reason for this behavior is provided by the presence of a duplicated Grb-2 binding site in its C-terminal tail (Y-1360 VNL-X_3-Y-1367 VNL). According to this hypothesis, it has been demonstrated that duplication of the Grb-2 binding site in Tpr-Met causes signalling reinforcement along the Ras pathway and enhances transformation (38).

Tpr-Ron may fail to transform host cells by its subcellular localization which is cytoplasmic, whereas the intact Ron receptor is located on the plasma membrane. This could lead to interaction with a different set of signalling and regulatory molecules, lacking the critical ones located in the inner face of the plasma membrane. This is however unlikely since Tpr-Met, which is cytoplasmic as well, is a powerful transforming agent. Moreover, we recently isolated a naturally occurring Ron variant, originated by alternative splicing, whose tyrosine kinase is activated by thiol-mediated oligomerization: this variant fails to transform fibroblasts in spite of its membrane localization (4).

Constitutive activation of Tpr-Ron, while inefficient in transformation did trigger a genetic program leading to the acquisition of an invasive phenotype. This program includes cytoskeletal reorganization, loss of intercellular junctions, cell dissociation (scattering) followed by active migration, and invasion of extracellular matrices (16, 55, 61). It has been shown that cell scattering is dependent on activation of Ras and Rac with concomitant inhibition of Rho (21, 40) and also requires phosphatidylinositol 3-kinase (PI 3-kinase) activation (8, 43). The Ras threshold required for the scattering response is by far lower than that necessary for growth and transformation (38). Tpr-Ron, in spite of its weak kinase, fulfills the requirements for activating cell scattering and matrix invasion and provides a naturally occurring example of dissociation between the two arms of the biological response triggered by the Met family of receptors.

The Ron and Met receptors, after controlled activation by their respective ligands, drive epithelial cells to migrate into collagen matrices, to proliferate, and to polarize. This complex regulation results in the formation of branched tubular structures (20). Tpr-Ron appears to be able to drive part of this program, inducing linear tubulogenesis but not branching. An interpretation of the failure of Tpr-Ron to complete tubulogenesis could be the cytosolic compartmentalization of the chimera that may alter the interactions with membrane-associated signal transducers. On the contrary, uncontrolled activation of Tpr-Met in MDCK cells boosts cell proliferation, as shown by the formation of larger spherical cysts, but fails to activate the morphogenic program. This is not in contrast to the constitutive scattering phenotype in these cells, since tubulogenesis is a complex mechanism based on the activation of multiple specific genes (3), while cell scattering is elicited by short-term signalling and is independent from RNA synthesis (40). The C-terminal swapped chimeras between Tpr-Met and Tpr-Ron indicate that the morphogenic phenotype is controlled exclusively by the intensity of the signal, rather than by specific signal transduction pathways. A potential explanation for the behavior of the Met kinase-based constructs could be that the high level of signalling conveyed by the Met kinase, optimal to induce unrestrained proliferation, interferes with the accomplishment of the morphogenic program. On the other hand, the low signalling threshold attained by the Ron kinase seems permissive and adequate to activate at least part of the morphogenic program. This can be explained by differential activation of critical genes due to a lower dosage of transcriptional activators induced by Ron. Interestingly, when MDCK cells are transfected with both Tpr-Met and Tpr-Ron constructs, the tubulogenesis is suppressed even in the presence of an active Tpr-Ron kinase. This suggests that the mitogenic signals elicited by the Met kinase are somehow dominant on the morphogenic signals elicited by Tpr-Ron.

In contrast with the above, Tpr-Sea, which was better than Tpr-Met in inducing transformation, elicited neither a fully invasive phenotype nor tubule formation. The docking site of Sea is made of two identical Y*VNL sequences, which can both bind Grb-2 at high affinity. This may prevent recruitment of the necessary amount of PI 3-kinase for promoting motility, invasion, and tubule formation. This is confirmed by recent data from our laboratory, obtained with a Tpr-Met mutant binding two Grb-2 molecules (and thus superactivating the Ras pathway) but lacking binding to PI 3-kinase. This mutant transformed the host cells with higher efficiency but was unable to trigger matrix invasion and metastasis, indicating that concomitant activation of the two pathways is necessary for the fully malignant phenotype (2, 15). Moreover, it has been shown that the lack of a functional PI 3-kinase binding site impairs the morphogenic response (8). Interestingly, in the tail of the naturally occurring aggressive oncogene v-*sea* (50) a C/A transversion substitutes the leucine residue at +3 to the first tyrosine (Y-1360) with a methionine residue, creating an optimal consensus for PI 3-kinase (Y-1360 INM), which may compensate for the presence of the asparagine residue at +2 (52).

Taken together, the data reported show that the *RON* gene codes for a potentially harmful receptor which may transduce invasive-metastatic signals but is hampered by an inefficient kinase domain. This suggests a possible role for activated Ron in tumor progression (late steps of malignancy) rather than in the early steps of the tumorigenic process.

ACKNOWLEDGMENTS

We thank Z. Zhen for technical suggestions in cell transformation assays and E. Medico for providing Sea antisera. We thank C. Ponzetto for critical comments and suggestions on the manuscript and for helpful discussion. The technical help of L. Palmas, G. Petruccelli, and R. Callipo is also acknowledged. We thank A. Cignetto and E. Wright for invaluable secretarial help.

This work was supported by grants from the Italian Association for Cancer Research to P.M.C. and to G.G. and the Italian National Research Council (CNR) (p.f. ACRO 94.01114.PF39 to P.M.C. and 94.01134.PF39 to G.G.). M.M.S., C.C. and S.G. are supported by fellowships from the Italian Association for Cancer Research.

REFERENCES

1. **Albini, A., Y. Iwamoto, H. K. Kleinman, G. R. Martin, S. A. Aaronson, J. M. Kozlowsky, and R. N. McEwan.** 1989. A rapid in vitro assay for quantitating the invasive potential of tumor cells. Cancer Res. **47:**3239–3245.
2. **Bardelli, A., E. Audero, M. L. Basile, F. Maina, S. Giordano, S. Ménard, P. M. Comoglio, and C. Ponzetto.** Submitted for publication.
3. **Barros, E., O. Santos, K. Matsumoto, T. Nakamura, and S. K. Nigam.** 1995. Differential tubulogenic and branching morphogenetic activities of growth factors: implications for epithelial tissue development. Proc. Natl. Acad. Sci. USA **92:**4412–4416.
4. **Collesi, C., M. M. Santoro, G. Gaudino, and P. M. Comoglio.** 1996. A splicing variant of the *RON* transcript induces constitutive tyrosine kinase activity and an invasive phenotype. Mol. Cell. Biol. **16:**5518–5526.
5. **Comoglio, P. M., and C. Boccaccio.** 1996. The HGF receptor family: unconventional signal transducers for invasive cell growth. Genes Cells **1:**347–354.
6. **Cooper, C. S., M. Park, D. G. Blair, M. A. Tainsky, K. Huebner, C. M. Croce,**

and G. Vande Woude. 1984. Molecular cloning of a new transforming gene from a chemically transformed human cell line. Nature (London) **311:**29–33.
7. **Cowley, S., H. Paterson, P. Kemp, and C. J. Marshall.** 1994. Activation of the MAP kinase is necessary and sufficient for PC12 differentiation and for transformation of NIH 3T3 cells. Cell **77:**841–852.
8. **Derman, M. P., M. J. Cunha, E. Barros, S. K. Nigam, and L. G. Cantley.** 1995. HGF-mediated chemotaxis and tubulogenesis require activation of the phosphatidylinositol 3-kinase. Am. J. Physiol. **268:**F1211–F1217.
9. **Dikic, I., J. Schlessinger, and I. Lax.** 1994. PC12 cells overexpressing the insulin receptor undergo insulin-dependent neuronal differentiation. Curr. Biol. **4:**702–708.
10. **Fixman, E. D., T. M. Fournier, D. M. Kamikura, M. A. Naujokas, and M. Park.** 1996. Pathways downstream of Shc and Grb2 are required for cell transformation by Tpr-Met oncoprotein. J. Biol. Chem. **271:**13116–13122.
11. **Gandino, L., P. Longati, E. Medico, M. Prat and P. M. Comoglio.** 1994. Phosphorylation of serine 985 negatively regulates the hepatocyte growth factor receptor kinase. J. Biol. Chem. **269:**1815–1820.
12. **Gaudino, G., V. Avantaggiato, A. Follenzi, D. Acampora, A. Simeone, and P. M. Comoglio.** 1995. The proto-oncogene RON is involved in development of epithelial, bone and neuro-endocrine tissues. Oncogene **11:**2627–2637.
13. **Gaudino, G., A. Follenzi, L. Naldini, C. Collesi, M. Santoro, K. A. Gallo, P. J. Godowski, and P. M. Comoglio.** 1994. *Ron* is a heterodimeric tyrosine kinase receptor activated by the HGF-homolog MSP. EMBO J. **13:**3524–3532.
14. **Gherardi, G., J. Gray, M. Stoker, M. Perryman, and R. Furlong.** 1989. Purification of scatter factor, a fibroblast-derived basic protein that modulates epithelial interaction and movement. Proc. Natl. Acad. Sci. USA **86:**5844–5848.
15. **Giordano, S., M. F. DiRenzo, Z. Zhen, M. Olivero, A. Bardelli, C. Ponzetto, and P. M. Comoglio.** Submitted for publication.
16. **Giordano, S., Z. Zhen, E. Medico, G. Gaudino, F. Galimi, and P. M. Comoglio.** 1993. Transfer of the motogenic and invasive response to scatter factor/hepatocyte growth factor by transfection of human *MET* proto-oncogene. Proc. Natl. Acad. Sci. USA **90:**649–653.
17. **Gonzatti-Haces, M., A. Seth, M. Park, T. Copeland, S. Oroszlan, and G. Vande Woude.** 1988. Characterization of the *TPR-MET* oncogene p65 and the *MET* proto-oncogene p140 protein tyrosine kinase. Proc. Natl. Acad. Sci. USA **85:**21–25.
18. **Graziani, A., D. Gramaglia, P. Dalla Zonca, and P. M. Comoglio.** 1993. Hepatocyte growth factor/scatter factor stimulates the Ras-guanine nucleotide exchanger. J. Biol. Chem. **268:**9165–9168.
19. **Greco, A., M. A. Pierotti, I. Bongarzone, S. Pagliardini, C. Lanzi, and G. Della Porta.** 1992. TRK-T1 is a novel oncogene formed by the fusion of *TPR* and *TRK* genes in human papillary thyroid carcinomas. Oncogene **7:**237–242.
20. **Gumbiner, B. M.** 1992. Epithelial morphogenesis. Cell **69:**385–387.
21. **Hartmann, G., K. Weidner, H. Schwarz, and W. Birchmeier.** 1994. The motility signal of scatter factor/hepatocyte growth factor mediated through the receptor tyrosine kinase Met requires intracellular action of Ras. J. Biol. Chem. **269:**21936–21939.
22. **Hayman, M. J., G. Kitchener, P. K. Vogt, and H. Beug.** 1985. The putative transforming protein of S13 avian erythroblastosis virus is a transmembrane glycoprotein with an associated protein kinase activity. Proc. Natl. Acad. Sci. USA **82:**8237–8241.
23. **Hill, C. S., and R. Treisman.** 1995. Transcriptional regulation by extracellular signals: mechanisms and specificity. Cell **80:**199–211.
24. **Honegger, A., T. J. Dull, D. Szapary, A. Komoriya, R. Kris, A. Ullrich, and J. Schlessinger.** 1988. Kinetic parameters of the protein tyrosine kinase activity of EGF-receptor mutants with individual altered autophosphorylation sites. EMBO J. **7:**3053–3060.
25. **Huff, J. L., M. A. Jelinek, C. A. Borgman, T. J. Lansing, and T. J. Parsons.** 1993. The proto-oncogene c*SEA* encodes a transmembrane protein tyrosine kinase related to the MET/HGF/SF receptor. Proc. Natl. Acad. Sci. USA **90:**6140–6144.
26. **Ishikawa, F., F. Takaku, M. Nagao, and T. Sugimura.** 1987. Rat c-*raf* oncogene activation by a rearrangement that produces a fused protein. Mol. Cell. Biol. **7:**1226–1232.
27. **Kato, J. Y., T. Takeya, C. Grandori, H. Iba, J. B. Levy, and H. Hanafusa.** 1986. Amino acid substitutions sufficient to convert the nontransforming $p60^{c\text{-}src}$ protein to a transforming protein. Mol. Cell. Biol. **6:**4155–4160.
28. **Kueng, K., E. Silfer, and V. Eppenbeger.** 1989. Quantification of cells cultured in 96-well plates. Anal. Biochem. **182:**16–19.
29. **Le Vea, C. M., J. N. Myers, W. C. Dougall, X. Qian, and M. I. Greene.** 1993. A structural and kinetic comparison of the proto-oncogenic and oncogenic neu holo-receptors expressed in insect cells. Receptor **3:**293–309.
30. **Li, B. Q., M. H. Wang, H. F. Kung, C. Ronsin, R. Breathnach, E. J. Leonard, and T. Kamata.** 1995. Macrophage-stimulating protein activates Ras by both activation and translocation of SOS nucleotide exchange factor. Biochem. Biophys. Res. Commun. **216:**110–118.
31. **Marshall, C. J.** 1995. Specificity of the receptor tyrosine kinase signaling: transient versus sustained extracellular signal-regulated kinase activation. Cell **80:**179–185.
32. **Medico, E., A. M. Mongiovì, J. Huff, M. A. Jelinek, A. Follenzi, G. Gaudino, J. T. Parsons, and P. M. Comoglio.** 1996. The tyrosine kinase receptors *Ron* and *Sea* control "scattering" and morphogenesis of the liver progenitor cells in vitro. Mol. Biol. Cell **7:**495–504.
33. **Montesano, R., K. Matsumoto, T. Nakamura, and L. Orci.** 1991. Identification of a fibroblast-derived epithelial morphogen as hepatocyte growth factor. Cell **67:**901–908.
34. **Nair, N., R. J. Davis, and H. L. Robinson.** 1992. Protein tyrosine activities of the epidermal growth factor receptor and ErbB proteins: correlation of the oncogenic activation with altered kinetics. Mol. Cell. Biol. **12:**2010–2016.
35. **Naldini, L., E. Vigna, R. Ferracini, P. Longati, L. Gandino, M. Prat, and P. M. Comoglio.** 1991. The tyrosine kinase encoded by the *MET* proto-oncogene is activated by autophosphorylation. Mol. Cell. Biol. **11:**1793–1803.
36. **Park, M., M. Dean, K. Kaul, M. J. Braun, M. A. Gonda, and G. Vande Woude.** 1986. Mechanism of *met* oncogene activation. Cell **45:**895.
37. **Ponzetto, C., A. Bardelli, Z. Zhen, F. Maina, P. Dalla Zonca, S. Giordano, A. Graziani, G. Panayotou, and P. M. Comoglio.** 1994. A multifunctional docking site mediates signalling and transforming by the hepatocyte growth factor/scatter factor receptor family. Cell **77:**261–271.
38. **Ponzetto, C., Z. Zhen, E. Audero, F. Maina, A. Bardelli, M. L. Basile, S. Giordano, R. Narsimhan, and P. M. Comoglio.** 1996. Specific uncoupling of the GRB2 from the Met receptor: differential effects on transformation and motility. J. Biol. Chem. **271:**14119–14123.
39. **Prat, M., R. P. Narsimhan, T. Crepaldi, M. R. Nicotra, P. G. Natali, and P. M. Comoglio.** 1991. The receptor encoded by the human c-*Met* oncogene is expressed in hepatocytes, epithelial cells and solid tumors. Int. J. Cancer **49:**323–328.
40. **Ridley, A. J., P. M. Comoglio, and A. Hall.** 1995. Regulation of the scatter factor/hepatocyte growth factor responses by Ras, Rac, and Rho in MDCK cells. Mol. Cell. Biol. **15:**1110–1122.
41. **Rodrigues, G. A., and M. Park.** 1993. Dimerization mediated through a leucine zipper activates the oncogenic potential of the *met* receptor tyrosine kinase. Mol. Cell. Biol. **13:**6711–6722.
42. **Ronsin, C., F. Muscatelli, M. G. Mattei, and R. Breathnach.** 1993. A novel putative receptor protein tyrosine kinase of the met family. Oncogene **8:**1195–1202.
43. **Royal, I., and M. Park.** 1995. Hepatocyte growth factor-induced scatter of Madin-Darby canine kidney cells requires phosphatidylinositol 3-kinase. J. Biol. Chem. **270:**27780–27787.
44. **Rush, J., and M. Levine.** 1994. Regulation of the dorsal morphogen by the *Toll* and torso signaling pathways: a receptor tyrosine kinase selectively masks transcriptional repression. Genes Dev. **8:**1247–1257.
45. **Sanger, F., S. Nicklen, and A. R. Coulson.** 1977. DNA sequencing with chain terminating inhibitors. Proc. Natl. Acad. Sci. USA **74:**5463–5467.
46. **Sawyers, C. L., and C. T. Denny.** 1994. Chronic myelomonocytic leukemia: tel-a-kinase what ets all about. Cell **77:**171–173.
47. **Shu, H. K., C. Chang, L. Ravi, L. Ling, C. M. Castellano, E. Walter, J. R. Pelley, and H. Kung.** 1994. Modulation of the erbB kinase activity and oncogenic potential by single point mutations in the glycine loop of the catalytic domain. Mol. Cell. Biol. **14:**6868–6878.
48. **Shu, H. K., J. R. Pelley, and H. Kung.** 1990. Tissue-specific transformation by epidermal growth factor receptor: a single point mutation within the ATP-binding pocket of the erbB product increased its intrinsic kinase activity and activates its sarcomagenic potential. Proc. Natl. Acad. Sci. USA **87:**9103–9107.
49. **Skeel, A., T. Yoshimura, S. D. Showalter, T. Tanaka, E. Appella, and E. L. Leonard.** 1991. Macrophage stimulating protein: purification, partial amino acid sequence and cellular activity. J. Exp. Med. **173:**1227–1234.
50. **Smith, D. R., P. K. Vogt, and M. J. Hayman.** 1989. The v-*sea* oncogene of avian erythroblastosis retrovirus S13: another member of the protein-tyrosine kinase gene family. Proc. Natl. Acad. Sci. USA **86:**5291–5295.
51. **Songyang, Z., and L. C. Cantley.** 1995. Recognition and specificity in protein tyrosine kinase-mediated signalling. Trends Biol. Sci. **20:**470–475.
52. **Songyang, Z., S. E. Shoelson, M. Chaudhuri, G. Gish, T. Pawson, W. G. Haser, F. King, T. Roberts, S. Ratnofsky, R. J. Lechleider, B. G. Neel, R. B. Birge, J. E. Fajardo, M. M. Chou, H. Hanafusa, B. Schaffhausen, and L. C. Cantley.** 1993. SH2 domains recognize specific phosphopeptide sequences. Cell **72:**767–778.
53. **Songyang, Z., S. E. Shoelson, J. Mcglade, P. Olivier, T. Pawson, X. R. Bustelo, M. Barbacid, H. Sabe, H. Hanafusa, T. Yi, R. Ren, D. Baltimore, S. Ratnofsky, R. A. Feldman, and L. C. Cantley.** 1994. Specific motifs recognized by the SH2 domains of Csk, 3BP2, fps/fes, GRB-2, HCP, SHC, Syk, and Vav. Mol. Cell. Biol. **14:**2777–2785.
54. **St. Johnston, D., and C. Nusslein-Volhard.** 1992. The origin of pattern and polarity in the Drosophila embryo. Cell **68:**201–219.
55. **Stoker, M.** 1989. Effect of scatter factor on motility of epithelial cells and fibroblasts. J. Cell. Physiol. **139:**565–569.
56. **Traverse, S., N. Gomez, H. Paterson, C. Marshall, and P. Cohen.** 1992. Sustained activation of the mitogen-activated protein (MAP) kinase cascade may be required for differentiation of the PC12 cells. Comparison of the effects of nerve growth factor and epidermal growth factor. Biochem. J. **288:**351–355.
57. **Traverse, S., K. Seedorf, H. Paterson, C. Marshall, P. Cohen, and A. Ullrich.** 1994. EGF triggers neuronal differentiation of PC12 cells that overexpress

the EGF receptor. Curr. Biol. **4:**694–701.
58. **Uehara, Y., and N. Kitamura.** 1992. Expression of a human hepatocyte growth factor/Scatter Factor cDNA in MDCK epithelial cells influences cell morphology, motility, and anchorage-independent growth. J. Cell Biol. **117:** 889–894.
59. **Wang, M.-H., A. Iwama, A. Skeel, T. Suda, and E. Leonard.** 1995. The murine *stk* gene product, a transmembrane protein tyrosine kinase, is a receptor for the macrophage-stimulating protein. Proc. Natl. Acad. Sci. USA **92:**3933–3937.
60. **Wang, M. H., C. Ronsin, M. C. Gesnel, L. Coupey, A. Skeel, E. J. Leonard, and R. Breathnach.** 1994. Identification of the *Ron* gene product as the receptor for the human macrophage stimulating protein. Science **266:**117–119.
61. **Weidner, K. M., J. Behrens, J. Vandekerckhove, and W. Birchmeier.** 1990. Scatter factor: molecular characteristics and effect of the invasiveness of epithelial cells. J. Cell Biol. **111:**2097–2108.
62. **Zhen, Z., S. Giordano, P. Longati, E. Medico, M. Campiglio, and P. M. Comoglio.** 1994. Structural and functional domains critical for constitutive activation of the HGF-receptor (*Met*). Oncogene **9:**1691–1697.